Proceedings of the 7th International Symposium on Cavitation
CAV2009
Aug 16-22, 2009, Ann Arbor, Michigan, USA

104

BUBBLE-SHOCK WAVE INTERACTION NEAR BIOMATERIALS

Siew-Wan Ohl
Institute of High Performance Computing
Singapore

Evert Klaseboer
Institute of High Performance Computing
Singapore

Boo Cheong Khoo
Mechanical Engineering, National University of Singapore
Singapore MIT Alliance
Singapore

ABSTRACT

The interaction of bubbles, both oscillating and stationary near bio-materials is of interest for the development of various medical treatment involving ultrasound and shock waves. This is because cavitation bubbles often nucleate in the bodily fluid under pressure waves, and their dynamics directly influence the success of the treatment and the collateral damages sustained. For example, in the treatment of Extracorporeal Shock Wave Lithotripsy (ESWL), cavitation bubbles are created when the shock wave is administered. These bubbles oscillate and collapse near the kidney stones and the body tissues. They are responsible both for the breaking up of the stones as well as the collateral damages to the nearby tissues. We study the interaction of an oscillating bubble near various bio-materials. The bio-materials are modeled as elastic fluids with similar physical properties such as elastic modulus, Poisson ratio, and density. The bubble dynamics are summarized based on bio-material physical properties. We also study the interaction of a stationary bubble with the nearby bio-materials when hit by a lithotripter shock wave. High speed jets and splitting of bubbles are observed due to the influence of the nearby biomaterials.

1. INTRODUCTION

The study of a stationary bubble near bio-materials in ultrasound has been studied by the authors [1]. In this study, we turn our attention to the interaction of a non-equilibrium bubble near the same set of bio-materials without the presence of an ultrasound field. In the later part of this study, we also investigate the interaction of a shock wave with such a bubble near bio-materials.

The motivation of this numerical study is fueled by the gaining popularity of the use of ultrasound equipments in medical treatment. Very often if the ultrasound is of high enough intensity, cavitation bubbles are incepted in the bio-fluids at the site of treatment. These bubbles are not in equilibrium and will oscillate and collapse in micro or milliseconds. The collapse of the bubbles may be important to the success of the treatment, but they are also responsible for collateral damages to the nearby tissues or bio-materials. However, it is known that oscillating bubble collapses in a different manner near different boundaries. Near a hard surface, the bubble tend to collapse with a high speed jet towards the surface [2,3,4]. A jet speed in the order of 100 m/s is observed for all bubble sizes. When a cavitation bubble collapses near a free surface, however, it tends to jets away from the air-water interface [5,6]. If the nearby interface is of intermediate 'hardness' between that of a solid boundary and a free surface, the bubble tends to exhibit complex behaviors, such as the formation of a 'mushroom bubble' and splitting into smaller bubbles before it collapses [7,8].

In this study, we summarize the bubble behaviors near a biomaterial modeled as an elastic fluid. The elastic fluid is of different density in comparison with water where the bubble is located. It is seen in the summary chart that the bubble might jet towards, split or jet away from the bio-materials depending on its density and elasticity. Also, we further extend the model to study how the bubble behaves near bio-material when it is hit by a shock wave. This might be of particular interests to researchers dealing with Extracorporeal Shock Wave Lithotripsy (ESWL) since cavitation bubbles from a previous shock might be interacting with a subsequent shock near kidney tissues. Detailed modeling of such scenario would be considered as future work.

2. MODELING AND SIMULATIONS

Details about the modeling and simulation of the bubble and the bio-materials using the Boundary Element Method can be found in previous articles from the authors [1,9]. A brief summary of the modeling and numerical method is given here.

In the domains of both water (where the bubble is in), and the nearby bio-material (as an elastic fluid), potential flow is assumed to be valid and thus a potential Φ_i can be introduced in the fluid which satisfies the Laplace equation

$$\nabla^2 \Phi_i = 0, \qquad (1)$$

where *i* equals to 1 for Fluid 1 (water), and 2 for Fluid 2 (bio-materials). The gradient of the potential gives the velocity vector $\underline{v}_i$

$$\underline{v}_i = \nabla \Phi_i, \qquad (2)$$

for both *i* = 1 and 2.

Furthermore the Bernoulli equation can be applied at the fluid-fluid interface on the side of Fluid 1 and the pressure p_1 can be expressed as:

$$p_1 = p_\infty(t) - \rho_1 \frac{D\Phi_{i1}}{Dt} + \frac{1}{2}\rho_1 |\underline{v}_1|^2. \qquad (3)$$

Here $Dx/Dt = \partial x/\partial t + \underline{v}_1 \bullet \nabla x$ represents the material derivative with respect to velocity $\underline{v}_1$. The subscript '*i*' in the potential refers to the fluid-fluid interface and ρ is the density. In a similar manner, the pressure at the fluid-fluid interface at the side of Fluid 2 is given as

$$p_2 = p_\infty(t) - \rho_2 \frac{D\Phi_{i2}}{Dt} + \rho_2 \underline{v}_2 \bullet \left(\underline{v}_1 - \frac{1}{2}\underline{v}_2 \right). \qquad (4)$$

The same material derivative with respect to $\underline{v}_1$ as used in (3) is employed here. This is done, since the nodes of the discretization of the fluid-fluid interface have been decided to move with Fluid 1 instead of Fluid 2. Furthermore Klaseboer and Khoo (2004b) have shown that for the pressure difference across the fluid-fluid interface can be modeled and expressed as

$$p_1 - p_2 = \frac{E}{2(1-\upsilon^2)R_0} h \qquad (5)$$

if Fluid 2 possess some elasticity. *E* is the elasticity modulus of Fluid 2 and *h* is the elevation of the fluid-fluid interface with respect to its initial equilibrium position. The Poisson ratio of Fluid 2 is indicated with υ.

The pressure at the bubble interface, p_b, is assumed to be equal to the uniform adiabatic pressure of the bubble interior throughout the simulation. The Bernoulli equation as applied to the bubble surface leads to

$$p_b = p_0 \left(\frac{V_0}{V} \right)^\gamma = p_\infty(t) - \rho_1 \frac{D\Phi_b}{Dt} + \frac{1}{2}\rho_1 |\underline{v}_b|^2. \qquad (6)$$

In (6), the subscript '*b*' refers to the bubble surface. The ratio of the specific heats of the bubble's contents is γ.

The normal velocities at the fluid-fluid interface are assumed to be opposite and equal. The Laplace equations at both fluids are solved using the Boundary element method as detailed in [1,2].

There are two important program input parameters for the bio-materials; the relative density (with respect to water), $\alpha = \rho_1/\rho_2$, and the dimensionless elasticity, $\kappa = E/(2(1-\nu^2)p_\infty)$, which is calculated from the Young's modulus (E) and Poisson ratio (ν) as shown in Table 1 [1].

Bio-material	Density (kg/m^3)	Young's modulus (kPa)	Poisson ratio	α	κ
Fat	950	5.6	0.45	1.05	0.037
Skin	1100	22.6	0.45	0.909	0.1288
Cornea	1400	47	0.49	0.714	0.2209
Brain	1000	240	0.495	1.0	1.589
Muscle	1060	790	0.45	0.943	4.673
Cartilage	1300	5000	0.4	0.769	22.89
Bone	2000	14000000	0.43	0.001	100.0

Table 1 The parameters used in the simulation for the various bio-materials. It is noted that the high Young's modulus value of bone tissue causes numerical difficulties. Therefore the bone is modeled as a solid wall as it is considered as a hard material. Justification and sources of the parameters in use can be obtained from a previous article by the authors [1].

3. RESULTS

3.1 Cavitation bubble interaction with bio-materials

This section studies the response of an oscillating cavitation bubble near various bio-materials with physical parameters as given in Table 1. All bubbles are set to an initial pressure (p_0) of 100 bar, and placed at a non-dimensionalized (by maximum bubble radius, R_{max}) stand-off distance, H' = 1.0 from the bio-material interface. This distance is chosen because if the bubble is placed too near to the bio-material, numerical instability in the calculation might affect the calculation and also the surface science interaction is not modeled here. If the bubble is placed too far from the bio-materials, it tends to oscillate many times before collapsing and therefore complicate the summary of the general bubble behavior near each bio-material. It is noted that the reference pressure, $p_\infty(t) = 1$ bar. Time is non-dimensionalized by $t_0 = R_{max}\sqrt{\rho_1/p_\infty}$.

Fig. 1 shows the bubble dynamics of the oscillating bubble near hard bio-materials such as cartilage tissue. The bubble moves towards the interface and collapses with a high speed jet (210 m/s). The same jetting behavior is seen for the bubble collapsing near cornea and bone (with jet speeds 206 and 78 m/s respectively). This can be explained by noting that cartilage tissue, cornea, and bone are considered as hard bio-materials. The oscillating bubble behaves similarly as it is near a solid boundary.

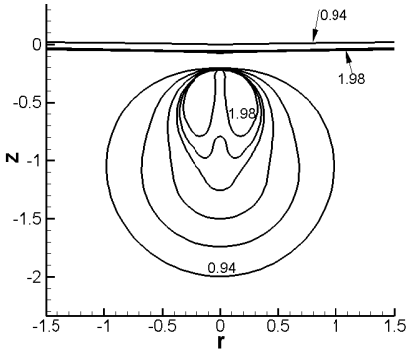

Fig. 1 Collapse profile of a cavitation bubble of initial pressure, p_0 = 100 bar, H′ = -1.0 away from the cartilage tissue. The dimensionless time, t′, for each profile from its maximum size (outermost) inwards are 0.94, 1.66, 1.84, 1.92, 1.94, and 1.98. The cartilage interface moves towards the bubble as it collapses.

If the bio-material near the bubble is rather soft, the bubble tends to split into two. In some cases, for example for a bubble next to some fat tissues (Fig. 2), the resulting bubbles from the split eventually jet away from one another. The fat interface, which was initially being pushed away as the bubble expands, moves slightly towards the bubble as it collapses. Similar splitting behavior is seen for a bubble collapsing near skin, brain, and muscle tissues. In all these cases, the bubble split into two before collapsing.

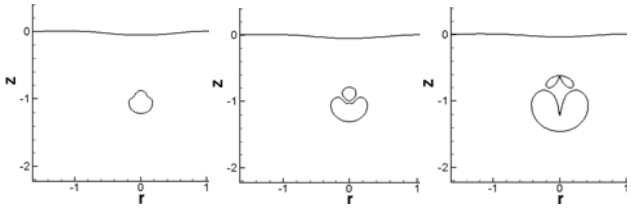

Fig. 2 Re-expansion phase (second period) of a cavitation bubble p_0 = 100 bar, H′ = -1.0 away from the fat tissue. The dimensionless time, t′, for each figure (left to right) are 1.96, 1.98, and 2.03. After splitting into two, the resulting bubbles collapse with opposite jets.

In summary, Fig. 3 shows the bubble response for a range of values of α and κ. The bubble is found to be jetting towards the elastic material if it is more than 1.4 times denser than water (i.e. $\alpha < 0.7$) for a wide range of κ. This means that an oscillating bubble tends to jet towards a dense interface with little regards to its elasticity. If the elastic material has a density of only 0.7 times that of water or less (i.e. $\alpha > 1.3$), and an elasticity related value κ less than 6, the bubble will collapse jetting away from it. Near this softer and lighter material, the bubble behaves similarly to when it is collapsing near a free surface. For materials with density close to water, including most of the bio-materials, the bubble tends to split into smaller bubbles, and exhibits complex behavior such as the resultant bubbles from the split jet away from one another.

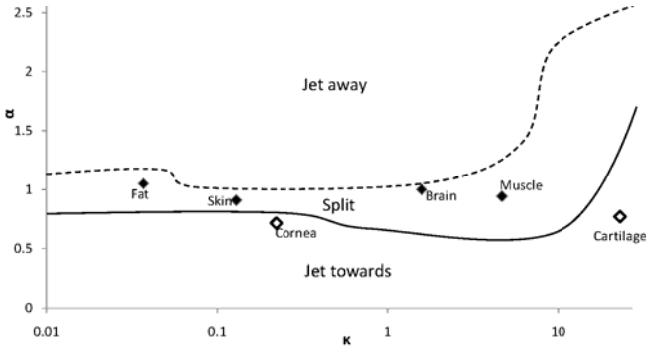

Fig. 3 Summary of bubble behaviour near an elastic material. The bubble is at H′ = -1.0 initially. The parameters ranges in consideration are α between 0.1 and 3.0, and κ between 0.01 and 27. This range encompasses all bio-materials mentioned previously except bone (indicated in the graph).

3.2 Bubble shock wave interaction near bio-materials

Besides oscillating bubbles, some pre-existing gas pockets and remnants bubbles from previous medical treatments might coalesce to form stationary bubbles (as in ESWL). It is also valuable to study the effect of the lithotripter shock wave on a stationary bubble. The shock wave is modeled as a traveling pressure wave through $p_\infty(t)$ in Eqn. (3) (details can be found in [10]), with profile as given by Fig. 1 in [11].

The shock hits the bubble from below. Bubbles between 10 to 100 μm in radius, collapse with a high speed jet towards all bio-materials. As shown in Fig. 4(a), the 10 μm bubble jets towards the fat tissue boundary with a jet speed of 1900 m/s. At the same time the fat tissue interface moves towards the collapsing bubble. Similar collapses are observed for all bio-materials, but the displacement of the bio-material interfaces vary. Soft bio-materials like fat move much towards the bubble while hard bio-material like cartilage hardly moves at all. Fig. 4(b) shows the collapse of a much larger stationary bubble (500 μm) hit by the same shock wave. It is noted that jets are observed from both the top and bottom surfaces of the bubble.

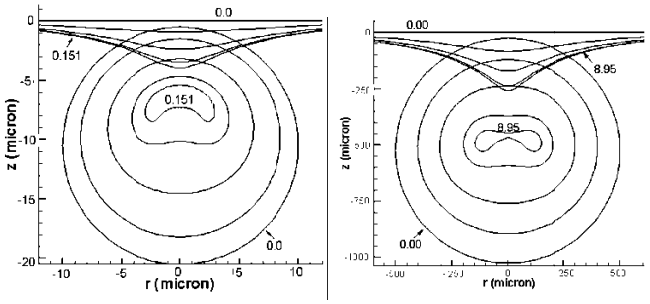

Fig. 4 The bubble shapes in time when (a) a 10 μm and (b) a 500 μm stationary bubble next to fat tissue (H' = 1.05 μm) is hit by a lithotripter shock wave shown in from the bottom. The time's for each bubble shape from its maximum size (outer most) to its collapse (inner most) are (a) 0.0, 0.112, 0.138, 0.148, and 0.151 μs, (b) 0.0, 3.57, 6.33, 8.15, and 8.95 μs.

Sometimes a very large bubble (e.g. 1 mm in radius) can form in vivo as a result of coalescence of many small bubbles. For this large bubble to be hit by the lithotripter shock wave, it does not collapse in its first period. It re-expands and then collapses in its second period by splitting into two (see Fig. 5).

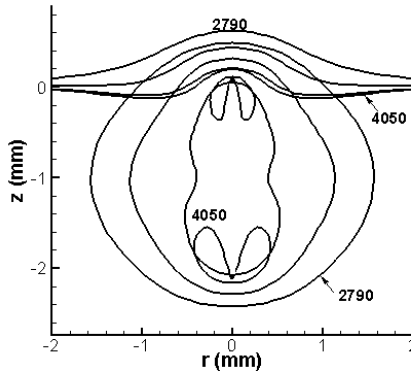

Fig. 5 The bubble shapes of a 1 mm bubble near (H′ = 1.05) fat tissue after it is hit by a shock wave. The bubble is at its second collapse phase. The time's for each bubble shape (outer to inner) are 2790, 3369, 3745, and 4050 μs.

For all other bio-materials (except bone), the bubble dynamics observed are similar. The shock wave is assumed to pass through the bio-materials without reflection because their acoustic impedances are close to that of water. However, for the case of bone, its acoustic impedance is about 5 times that of water, and the reflection of the shock wave is therefore considered. As shown in Fig. 6, the reflected shock travels downwards from the interface causes the bubble to collapse faster at 0.156 μs (as compared to 0.166 μs when reflection is not modeled), and with a higher jet speed of 1430 m/s (as compared to 808 m/s without considering reflection).

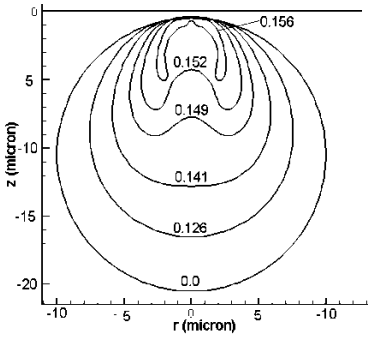

Fig. 6 The bubble shapes of a 10 μm bubble collapsing next to a bone interface. The respective time (in μs) for each bubble shape are indicated.

4. CONCLUSION

Interaction of an oscillating bubble near various boundaries (solid [2, 3, 4], free surface [5, 6], elastic materials [7, 8], and composite surfaces [12]) has been of great research interest. We contribute to the wealth of knowledge on bubble-interface interaction by summarizing general bubble behaviors near bio-materials of different density and elasticity. Interesting phenomena were observed. For hard biomaterials, such as cartilage, cornea, and bone, the bubble tends to jet away from the interface. For other bio-materials, the bubble tends to split into two smaller bubbles before collapsing with jets away from one another. For elastic materials that are soft and light, the nearby bubble will jet away from the elastic materials.

Apart from an oscillating bubble, we also investigated how a stationary bubble behaves when hit by a shock wave near a bio-material. Bubbles of different initial sizes were investigated. For this particle shock wave profile (Fig. 1 in [11]), small bubbles (< 500 μm) tend to jet towards the elastic interface as it moves towards the bubble. A very high speed jet (1900 m/s) is resulted. For large bubbles, such as a 1 mm in radius bubble, the shock wave will cause it to split into two smaller bubbles before they jet away from one another.

References

[1] Fong, S.W., Klaseboer, E., Turangan, C.K., Khoo, B.C., Hung, K.C. 2006 Numerical analysis of a gas bubble near bio-materials in an ultrasound field. *Ultrasound Med. Bio.* **32**, 925-942.

[2] Blake, J.R., Taib, B.B., and Doherty, G. 1986 Transient cavities near boundaries. Part 1. Rigid boundary. *J. Fluid Mech.* **170**, 479-497.

[3] Lauterborn, W., and Bolle, H. 1975 Experimental investigations of cavitation bubble collapse in the neighbourhood of a solid boundary. *J. Fluid Mech.* **72**, 391-399.

[4] Tomita, Y. and Shima, A. 1990 High-speed photographic observations of laser-induced cavitation bubbles in water. *Acustica* **71**, 161-170.

[5] Chahine, G.L. 1977 Interaction between an oscillating bubble and a free surface. *Trans. ASME I: J. Fluids Eng.* **99**, 709-716.

[6] Blake, J.R., Taib, B.B., and Doherty, G. 1987 Transient cavities near boundaries. Part 2. Free surface. *J. Fluid Mech.* **181**, 197-212.

[7] Brujan, E.A., Nahen, K., Schmidt, P., and Vogel, A. 2001a Dynamics of laser-induced cavitation bubbles near an elastic boundary. *J. Fluid Mech.* **433**, 251-281.

[8] Turangan, C.K., Ong, G.P., Klaseboer, E., and Khoo, B.C. 2006 Experimental and numerical study of transient bubble-elastic membrane interaction. *J. Appl. Phys.* **100**, 054910.

[9] Klaseboer, E., and Khoo, B.C. 2004 An oscillating bubble near an elastic material. *J. Appl. Phys.* **96**, 5808-5818.

[10] Klaseboer, E., Fong, S.W., Turangan, C.K., Khoo, B.C., Szeri, A.J., Calvisi, M.L., Sankin, G.N., and Zhong, P. 2007 Interaction of lithotripter shockwaves with single inertial cavitation bubbles. *Journal of Fluid Mechanics*, **593**, 33-56.

[11] Sankin, G.N. and Zhong P. 2006 Interaction between shock wave and single inertial bubbles near an elastic boundary. *Physical Review E*, **74**, 046304.

[12] Tomita, Y. and Kodama, T. 2003 Interaction of laser-induced cavitation bubbles with composite surfaces. *J. Appl. Phys.* **94**, 2809-2816.